

Fluctuation kinetics of an isolated Ag(110) step

W. W. Pai* and N. C. Bartelt†

Department of Physics, University of Maryland, College Park, Maryland 20742

J. E. Reutt-Robey

Department of Chemistry, University of Maryland, College Park, Maryland 20742

(Received 18 December 1995; revised manuscript received 28 February 1996)

We study the equilibrium thermal fluctuations of a Ag(110) step at room temperature with scanning tunneling microscopy. By employing a Langevin analysis, step fluctuations are shown to be determined by adatoms exchanging between terraces and steps, and the room-temperature detachment rate from steps is estimated to be 3 atoms/s per step site. The mass transport mechanism at steps and the efficiency of the step as an adatom source bear directly on the kinetics of surface reactions that involve the participation of substrate atoms. We will briefly discuss the O/Ag(110) system as an example. [S0163-1829(96)06223-6]

I. INTRODUCTION

A step is a quite common defect on macroscopically “flat” surfaces. Higher step densities can be easily obtained by orienting the surface normal off low-Miller-index directions. Since steps are natural sources and sinks of atoms, they play an important role in surface chemical processes such as diffusion, nucleation, and growth. Recently, with the rapid advances of *in situ* real-time imaging techniques, such as reflection electron microscopy,^{1,2} low-energy electron microscopy,^{3–5} atomic force microscopy,⁶ and high-speed scanning tunneling microscopy (STM),^{7,8} it has become feasible to study directly the kinetics of step motion. The study of the step kinetics will shed light on such important processes as crystal growth and the realization of equilibrium surface structures.

A fundamental aspect of step motion is the step position fluctuations caused by equilibrium thermal excitations. Step edges often appeared “frizzled” in STM images^{9–12} due to the motion of atoms at step edges on a time scale faster than the scanning process. Step fluctuations can be recorded and analyzed to obtain the fundamental mass transport mechanisms and the rate of motion at step edges.^{8,13–15} The experimental feasibility of this approach has been demonstrated by several studies. For example, atoms are shown to exchange predominantly between steps and terraces on Si(111) at elevated temperature (900)°,¹³ whereas atoms are mainly hopping along step edges on vicinal Cu(100) (Refs. 16 and 17) at room temperature. The density and mobility of adatoms on the terraces increase as temperature increases, causing increased rates of exchanges with step edges. However, these attachment and detachment processes can even occur at room temperature, as observed recently on Au(110).¹⁸ Furthermore, the step mobility caused by adatom exchange is sufficient to allow the rapid thermodynamic faceting of Ag(110) induced by the formation of oxygen added row structure.¹⁹

In this paper we use STM and apply the Langevin formalism to study the step fluctuations on a clean Ag(110) surface at room temperature. In contrast to previous STM studies of step fluctuations,^{8,16,18} we analyze the fluctuations of a large segment of the step edge, in addition to the fluctuations of a

single step site. The possible complications of the mass exchange and step-step interactions between steps are effectively eliminated by choosing an “isolated” step that is at least 3000 Å away from neighboring steps. The dominant mass transport mechanism at the Ag(110) step edge is shown to be the exchange of adatoms between steps and terraces, rather than diffusion along the step edge. The rate limiting step of the observed step fluctuations is found to be the probability for the attachment/detachment event itself, rather than diffusion on the adjoining terraces to and from the step edge. An appreciable rate of step-edge detachment, ~ 3 atoms/s per step site, reveals the step as an efficient source of Ag adatoms. This mass transport mechanism at steps has immediate implications for surface chemical processes. For example, the mobile adatoms in equilibrium with the step edge may influence chemisorption dynamics, adlayer formation, or even reaction mechanism. As will be observed for O/Ag(110), mobile Ag adatoms foster the formation of the “added-row” O/Ag(110) structure.^{20–22}

The remainder of this paper is organized as follows: Experimental procedures are described in Sec. II. A review of the Langevin theory of step fluctuations follows in Sec. III. Results obtained for an isolated Ag(110) step will then be presented in Secs. IV and V.

II. EXPERIMENT

The chamber setup and cleaning procedure of the Ag(110) sample used in the experiments are described elsewhere.²¹ The step fluctuations were investigated by STM (Omicron STU-052) under ultrahigh vacuum conditions. To study the intrinsic step fluctuations, an isolated step is chosen to minimize the perturbations (entropic and energetic step-step interactions, mass exchange) from the neighboring steps. We have been able to locate steps routinely with terrace widths exceeding 1000 Å on a macroscopic Ag(110) surface region (~ 5 mm across). We restrict observations to steps that are at least 3000 Å away from the neighboring steps. Such an isolated step must also be able to fluctuate freely, and thus not be pinned by impurities or dislocations intersecting the surface in any way.

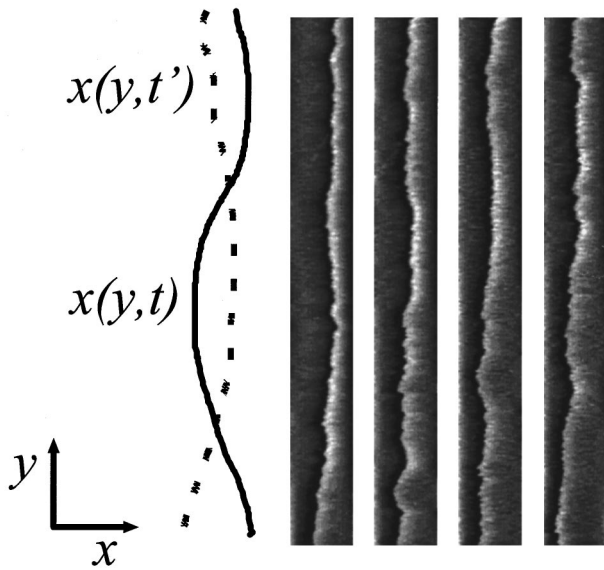


FIG. 1. The displacement x of a step is expressed as a function of step position y and time t : $x = x(y, t)$. As shown schematically, the position of the step at time t (solid line) could differ substantially from the step position at time t' (dashed line). Four $600 \text{ \AA} \times 5000 \text{ \AA}$ STM images, each accumulated in 18 s of a fluctuating isolated step are shown at 30-min intervals. From a Fourier analysis, the mass transport mechanism at step edges is shown to be atomic exchange between steps and terraces.

Two approaches are used to analyze the step fluctuations. One approach is to analyze the fluctuations of a single position along the step edge; another approach is to analyze fluctuations of a large step-edge segment. For the single point analysis, images were taken with the tip scanning *perpendicularly* to the step edge along the *same* line repeatedly. This type of image is termed a “time” image because the y axis represents a temporal, rather than spatial, coordinate.¹⁶ We acquired the time images with a typical size of $300 \text{ points} \times 6000 \text{ points}$, presetting a spatial resolution of $x = 1.0 \text{ \AA} / \text{pixel}$ and a temporal resolution of $y = 100$ (or 200) $\mu\text{s} / \text{pixel}$. To obtain fluctuation data for whole-segment analysis, we took a sequence of “conventional” gray scale images of the same isolated step, as shown in Fig. 1. Each $600 \text{ \AA} \times 5000 \text{ \AA}$ image was acquired in 18 s with spatial resolutions of $x = 2 \text{ \AA} / \text{pixel}$ and $y = 20 \text{ \AA} / \text{pixel}$. Since the step fluctuates with time, the step positions can be decomposed to allow the study of individual fluctuating Fourier components. About 600 continuously scanned STM images were analyzed to obtain the time evolution of the Fourier components of the isolated step. To obtain the step-edge positions, the scan lines (perpendicular to step) are fitted to a phenomenological functional form $a_0 + a_1 x + a_2 \tanh[(x - a_3)/w]$, where a_3 denotes the step-edge position. A typical fit is shown in Fig. 2.

III. THEORETICAL BACKGROUND: LANGEVIN THEORY OF STEP FLUCTUATIONS

The basic idea of the Langevin analysis is that the observable macroscopic motion is caused by the sum of many random unobservable microscopic events. For example, the

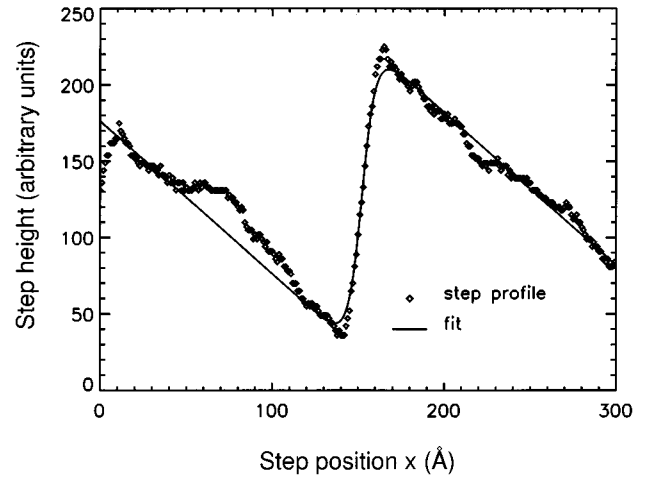


FIG. 2. A typical step profile of single scan line in the “time” image. The profile is fitted to a functional form, $a_0 + a_1 x + a_2 \tanh[(x - a_3)/w]$, where a_0 , a_1 , a_2 , and a_3 are fitting parameters. The step position a_3 might be shifted with different choices of initial fitting parameters. However, this shift is a systematic error and is canceled in the autocorrelation $G(t - t') = \langle |x(t) - x(t')|^2 \rangle$.

Brownian motion of a particle is caused by numerous molecular collisions. Such an analysis is appropriate for STM data when the step fluctuations are caused by extremely rapid microscopic events such as thermal kink formations and atomic detachments and/or attachments. In the Langevin theory for step fluctuations,¹⁵ random thermal noise roughens the step edge, while the step positions are assumed to diffuse towards lower free energy with a speed proportional to the free-energy gradient. Supposing the step position x can be expressed as a function of position y along the step edge, $x = x(y, t)$, as shown in Fig. 1, the step dynamics are then governed by

$$\frac{\partial x(y, t)}{\partial t} = -\frac{\Gamma_a}{kT} \frac{\delta H}{\delta x} + \eta(y, t), \quad (1)$$

where Γ_a represents the step mobility, k the Boltzmann constant, H the Hamiltonian for the step, and $\eta(y, t)$ the thermal noise. If one assumes the step moves in a quadratic potential cx^2 (as determined by a $1/d^2$ repulsive step-step interaction with the value c determined by the strength of step-step interaction) and the step stiffness is $\tilde{\beta}$, the Hamiltonian of the step is then the sum of the energy associated with bending the step and the step interaction energy, $H = \int [\frac{1}{2} \tilde{\beta} (\partial x / \partial y)^2 + cx^2] dy$ when the bending is small. Opposing the step relaxation term is a random noise term $\eta(y, t)$ caused by thermal excitations in step edges. There are several important microscopic mechanisms that can cause step motion. We concentrate on one special case (a), the step-terrace exchange case, in which adatoms (vacancies) exchange between step edges and terraces and contrast the behavior of model (a) with case (b), the step-hopping case, in which atoms hop from step site to another along the *same* step edge. We shall assume the step is under thermal equilibrium. In case (a) the noise $\eta(y, t)$ is uncorrelated [i.e., $\eta(y, t)$ does not have “memory” in either time or

space] and satisfies the condition $\langle \eta(y,t)\eta(y',t') \rangle = 2(\Gamma_a/kT)\delta(y-y')\delta(t-t')$. The functional derivative of Eq. (1) leads to

$$\frac{\partial x}{\partial t} = \frac{\Gamma_a \tilde{\beta}}{kT} \frac{\partial^2 x}{\partial y^2} - 2 \frac{\Gamma_a c x}{kT} + \eta(y,t). \quad (2)$$

In case (b), the noise term $\eta(y,t)$ is correlated because atoms are hopping from one site to another. Since mass transport for the step-hopping case occurs only along the step edge, the mean step position $\int x dy$ is fixed. Intuitively, one expects a step to approach equilibrium much more slowly in case (b) than in case (a). In fact, the time dependence of thermal equilibrium fluctuations in cases (a) and (b) also exhibits different behaviors. The autocorrelation function for the same step site at different times, $G(t-t') = \langle [x(t) - x(t')]^2 \rangle$, is the mean square deviation of the step position. For the step-terrace exchange case (a), the initial time dependence of the autocorrelation scales as $|t-t'|^{1/2}$.¹⁵

$$G(|t-t'|) = \left(\frac{16kT\Gamma_a}{\pi\tilde{\beta}} \right)^{1/2} |t-t'|^{1/2}. \quad (3)$$

For the step-hopping case (b), the autocorrelation scales as $|t-t'|^{1/4}$. The scaling behavior of the initial time dependence of this autocorrelation function can be used to distinguish the dominant mass transport mechanism at step edges.

A complementary, but more in-depth approach is to analyze fluctuations by examining the step in Fourier space, as one would do with a vibrating string. Long-wavelength fluctuations in the step edge are observed to decay slowly because they require a large amount of mass, while short-wavelength fluctuations decay quickly. It is thus natural to study the time dependence of the Fourier components of the step-edge positions. We first decompose the step position x into time-dependent Fourier components:

$$x(y,t) = \sum_q x_q(t) e^{iqy}, \quad (4)$$

where q represents the Fourier wave vectors. The autocorrelation function for each Fourier amplitude x_q at different times can be defined accordingly as $G_q(|t-t'|) = \langle [x_q(t) - x_q(t')]^2 \rangle$, leading to an exponential saturation of $G_q(t)$:

$$G_q(t) = \frac{2kT}{L(\tilde{\beta}q^2 + 2c)} \left(1 - \exp\left[-\frac{t}{\tau(q)}\right] \right), \quad (5)$$

where L is the length of the analyzed step and $\tau(q)$ is a characteristic time constant.

For the isolated step of our study, the interaction strength c in Eq. (5) is negligible. The exponential saturation amplitude of $G_q(t)$ is thus inversely proportional to q^2 , independent of the mass transport mechanism. For the adatom detachment/attachment case (a), the time constant $\tau(q)$ scales as q^{-2} ,

$$\tau(q) = \frac{kT}{\Gamma_a(\tilde{\beta}q^2 + 2c)} \approx \frac{kT}{\Gamma_a \tilde{\beta}q^2}, \quad (6)$$

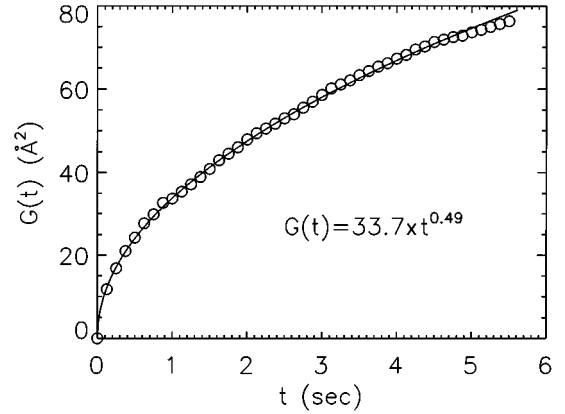


FIG. 3. From a STM “time” image of a point along the step edge, $x(t)$, the autocorrelation function $G(t) = \langle [x(t) - x(0)]^2 \rangle$ is evaluated (circles) and fit to $G = at^x$. The fit (solid line) shows the function scales as $t^{1/2}$ up to $G(t)^{1/2} \sim 9 \text{ \AA}$, indicating the step-edge fluctuations are caused by thermal exchange of atoms between steps and terraces. The best fit value for this measurement is $G(t) = (37.8 \pm 0.1)t^{0.492 \pm 0.002} (\text{\AA}^2)$. The average of 5 independent measurements gives $G(t) = (36 \pm 4)t^{0.46 \pm 0.03} \text{\AA}^2$.

whereas for the kink motion case (b), $\tau(q)$ scales as q^{-4} .

To summarize this Langevin analysis of equilibrium step fluctuations, the time dependence of the autocorrelation function $G(t)$ and/or the q dependence of the time constant $\tau(q)$ can be used to distinguish the two extreme mass transport mechanisms: step-terrace exchange and step-restricted hopping. Step stiffness $\tilde{\beta}$, and the step mobility Γ_a [or hopping rate Γ_h (Ref. 15)] are also obtained.

IV. RESULTS AND ANALYSIS

The isolated step used extensively for our analysis is shown in Fig. 1. A typical plot of the autocorrelation function $G(t)$ obtained from a time image of a single point along this step edge appears in Fig. 3. Upon fitting this function to the power law at^x , we obtain $G(t) = (36 \pm 4) (\text{\AA}^2)t^{0.46 \pm 0.03}$. We have measured the autocorrelation with different scanning speeds (100 and 200 $\mu\text{s}/\text{pixel}$) and different tunneling conditions (-1.4 – 3.0 V sample bias, 1.0–2.0-nA tunneling current), and the calculated autocorrelation function $G(t)$ shows no systematic change with these tunneling parameters. The gap resistance under these tunneling conditions is greater than $10^9 \Omega$. This resistance is three orders of magnitude larger than that typically used for STM manipulation of surface atoms or molecules.^{23–25} We thus assume that the tip does not affect the magnitude of step fluctuations, despite repetitive scanning of the same step-edge point.

The time exponent for $G(t)$ is close to $\frac{1}{2}$, strongly suggesting that mass transport on clean Ag(110) is via the step-terrace exchange mechanism [see Eq. (3)]. The ± 0.03 error in the exponent of the autocorrelation function $G(t)$ warrants further discussion. We first emphasize that the exponents were extracted from the short-time behavior of the autocorrelation ($t < 6$ s).¹⁵ In general the exponent is expected to decrease at longer times when the fluctuations become limited as the amplitude becomes comparable to the terrace width. However, the nanoscale fluctuations of the isolated

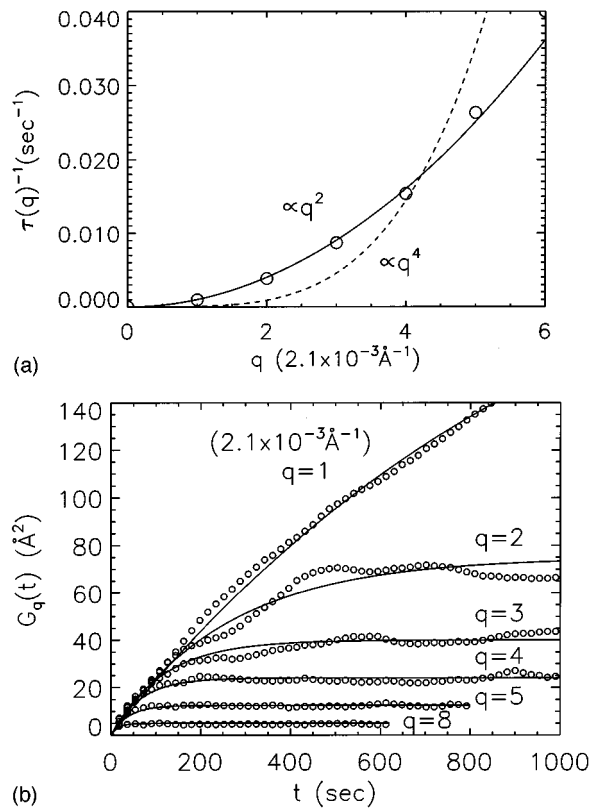


FIG. 4. (a) Fourier decomposition of the motion of an isolated step. The autocorrelation functions $G_q(t)$ for different Fourier components q (circles) together with exponential fits (lines). The exponential saturation values for $G_q(t)$ scale as q^{-2} , permitting estimate of the step stiffness $\bar{\beta}$. The wave vector $q=1$ corresponds to a wavelength of 3000 \AA . (b) The saturation values for the autocorrelation $G_q(t)$ plotted against q reveal the characteristic time $\tau(q)$. The reciprocal of the time constant, $\tau(q)^{-1}$, is fitted to a q^2 dependence [solid line, for step motion via step-terrace exchange, $\tau(q)^{-1} = (1.00 \pm 0.06) \times 10^{-3} q^2$] and to a q^4 dependence [dashed line, for step motion via kink movements, $\tau(q)^{-1} = (1.0 \pm_{-0.7}^{3.0}) \times 10^{-4} q^4$]. Only the q^2 form yields a good fit, and from the fitting prefactor the average time between successive detachments is found to be ~ 210 ms.

step in our experiment are much smaller than the terrace width ($\sim 3000 \text{ \AA}$) at time $t < 6$ s. The small deviation of the exponent from $\frac{1}{2}$ thus cannot be explained by the general trend mentioned above. Two other factors could lower the exponent. The contribution of the apparent fluctuations from kink motion increases at longer times. This is because the possibility for kinks to move across the scanning line by step hopping is larger at longer time separation.²⁶ For large magnitude (and long wavelength) fluctuations, the time scale of the fluctuations becomes limited by diffusion in the adatom sea: step fluctuations are slowed because the locally high densities of adatoms near the step edge cannot diffuse away quickly. The time exponent for the autocorrelation function in this case would be $\frac{1}{3}$ rather than $\frac{1}{2}$.^{27,28}

Turning now to a fluctuating step segment, the computed time correlation $G_q(t)$ is shown in Fig. 4(a), along with the fits to the exponential functional form of Eq. (5). Clearly, the fluctuations with longer wavelengths (small q) decay slower than the fluctuations with shorter wavelengths (large q). The

inverse of the time constant, $\tau(q)^{-1}$, also scales more consistently with a q^2 dependence than with a q^4 dependence as shown in Fig. 4(b). From Eq. (6), the q^2 proportionality to $\tau(q)^{-1}$ implies, again, that the dominant mass transport mechanism is by exchanging adatoms between steps and terraces.

Values for the step mobility Γ_a can be obtained along with the step fluctuation mechanism. The step mobility is a measure of how the net position of the step relaxes towards equilibrium. From a fit of the amplitudes of the autocorrelation function $G_q(t)$ to Eq. (5), we determine the step stiffness $\bar{\beta} \approx kT/1.4 \text{ \AA}^{-1}$, i.e., $\bar{\beta} \approx 18 \text{ meV/\AA}$, for this 30° $[1\bar{1}0]$ step. We evaluate the step mobility Γ_a from the best fit of the autocorrelation $G(t)$ to Eq. (3), obtaining $\Gamma_a = 1.8 \times 10^2 \text{ \AA}^3 \text{ s}^{-1}$. Alternatively, the step mobility can also be obtained from the Fourier analysis, as per Eq. (6). As shown in Fig. 4(b), we find $\Gamma_a = 3.0 \times 10^2 \text{ \AA}^3 \text{ s}^{-1}$, in reasonable agreement with the value obtained from Eq. (3).

Since the step mobility Γ_a describes how a step diffuses towards the equilibrium position, Γ_a can be related to atomic dimensions and the microscopic time scale by assuming the underlying microscopic mechanism is the random attachment and detachment of single atoms. In this case, $\Gamma_a \approx a^3/\tau_a$, where a is an atomic dimension ($\sim 4 \text{ \AA}$ for Ag) and τ_a is the mean time between successive attachments or detachments at an arbitrary step site. Using $\Gamma_a = 1.8 \times 10^2 \text{ \AA}^3 \text{ s}^{-1}$, we deduce $\tau_a \approx 350$ ms. This mean attachment/detachment time is significant. A substantial number of Ag adatoms, ~ 3 atoms/s per site, are exchanging between steps and terraces. Since this exchange rate is not limited by terrace diffusion,²⁸ the steps are thus easily able to maintain an equilibrium concentration of adatoms on terraces.

We note that the results described above are for a step rotated 30° from the $[1\bar{1}0]$ direction. The effect of geometric kinks on these transport parameters must thus be questioned. We have also analyzed the step fluctuations on an isolated step running in the close-packed $[1\bar{1}0]$ direction. Following the same analysis discussed above, we obtain the step stiffness $\bar{\beta} \approx 6kT \text{ \AA}^{-1}$ and a mean detachment/attachment time $\tau_a \approx 400$ ms. This exchange rate is quite close to that obtained for the 30° $[1\bar{1}0]$ isolated step, indicating the ability for steps to supply Ag adatoms onto terraces does not depend appreciably on the step orientation, and thus kink density, at room temperature. Since kink sites should provide energetically preferred sites for step-terrace adatom exchange,¹⁸ it is surprising that the exchange rate exhibits little dependence upon orientation (e.g., kink density) of the step edge. A high density of thermally excited kinks on all step orientations could account for this observation.

V. DISCUSSION

The exchange rate between steps and terrace, 3 s^{-1} , is high enough that it suggests that an equilibrium concentration of Ag adatoms can be easily maintained by the facile step-terrace site exchange, even at room temperature. What are the implications of this significant step-terrace exchange rate? A number of chemisorption systems are known to exhibit overlayer structures in which the density of substrate atoms in the adsorbate binding layer differs significantly

from that of the original surface.²⁹ For example, the (2×1) -O/Cu(110) system adopts an “added-row” structure in which the Cu adatom density in the top layer is 0.5 ML.³⁰ The overlayer formation kinetics and the role of steps in the processes involving substrate atoms are very interesting problems. We have studied the relation between the mass transport at step edges and the oxygen overlayer formation in O/Ag(110).²⁰ Briefly, the oxygen overlayer is also an “added-row” structure that incorporates extra Ag atoms. As we will show in the accompanying paper,²¹ this rate of thermal detachments and attachments, ~ 3 Ag atoms/s per site, is sufficient to supply Ag atoms to form the added-row reconstruction when the oxygen partial pressure is low. The kinetic balance between the supply rate from steps and the reaction rate of oxidation on terraces, however, cannot be maintained if the oxygen pressure exceeds a critical value $P_c \approx 10^{-5}$ mbar. The step source of Ag is then supplemented by vacancy-island formation on the terraces.

Finally, we comment on the validity of using serially obtained STM images as an experimental probe of step motion. To study best the real-time thermal fluctuations of steps, two competing factors must be considered. One is to have a fast image acquisition rate and the other is to get a high spatial resolution. The *in situ* real-time imaging techniques, such as reflection electron microscopy and low-energy electron microscopy, collect larger images at a faster video rate (> 10 frames/s) than conventional STM’s.³¹ However, the highest spatial resolution of these techniques is on the order of nanometers. Scanning tunneling microscopy, in contrast, achieves sub-Å spatial resolution. A compromise between time and spatial resolutions thus has to be made, specific to the system of interest. A conventional STM has proven sufficient to study the room-temperature step fluctuations on this noble metal surface. First, the nominal amplitude of step fluctuations for metal surfaces such as Ag(110) at room temperature is usually less than 10 Å. This small amplitude is easily accessible to STM, but problematic for electron microscopy. Second, the STM images acquired (image acquisition time of 18 s in this study) still represent “snap shots” of the step configuration: Let us consider the lowest Fourier component of the step fluctuations, i.e., the fluctuation with a wavelength equal to the length of the analyzed step segment. If the time required for this fluctuation to complete one period is much larger than the time required for taking one STM image, the consecutive STM images will be nearly identical and the single STM image can be viewed as “snap shot.” Comparing the 18-s duration of one STM frame to the 1000-s relaxation time of the longest-wavelength Fourier component,³² we find a 1/50 ratio that is indeed small. We thus demonstrate that it is possible to use a conventional “low-speed” STM to study the room-temperature thermal fluctuations on metal surfaces.

VI. CONCLUSION

A Langevin analysis is applied to the thermal fluctuations of an isolated Ag(110) step, as viewed by STM. The domi-

nant mass transport mechanism at the step edge is shown to be the exchange of adatoms between steps and terraces. A microscopic time τ_a , describing the average time between successive detachments (or attachments) at an auxiliary step edge site, is about 350 ms. A substantial number of Ag adatoms, ~ 3 atoms/s per site, can detach from step edges even at room temperature, making the step an efficient source of Ag adatoms. Steps thus serve as a ready supply of mobile adatoms, even at room temperature. This has important implications for surface chemistry. One such example, involving an Ag adatom incorporated into a complex overlayer structure with chemisorbed oxygen, is presented in the following paper.²¹

Note added in proof. Because of the large step mobility reported in this paper, step structure is very susceptible to modification. One example of this susceptibility is the rapid oxygen-induced faceting described in Ref. 19; another is that step structure can be modified by the scanning STM tip. Operating at a reduced gap resistance ($0.04 \times 10^9 \Omega$) and higher sampling densities, Li, Berndt, and Schneider²⁴ observed the formation of large tip-induced protrusions in the position of a step edge. Such effects are strongly affected by the distance between adjacent scan lines and the scan angle with respect to $[1\bar{1}0]$. Scanning perturbations were minimized in our experiments by employing a large gap resistance ($> 10^9 \Omega$), scanning at low sampling densities (as low as 20 Å/line), and by investigating isolated steps at most 30° off $[1\bar{1}0]$. Under these conditions, no systematic changes in step structure due to scanning were observed. Thus, we are confident that the fluctuations we observe are predominantly due to intrinsic equilibrium thermal fluctuations. It is clear that scanning perturbations can readily make changes in step structure which are already thermally accessible. Indeed, the tip-assisted formation of large step protrusions without the formation of vacancies of equivalent nearby areas indicates that nearby steps must be efficient adatom sources and thus have large natural equilibrium thermal fluctuations. The time required for such a tip-induced protrusion to decay thermally to a straight step confirms our quantitative conclusions about step mobility and the efficiency of steps as adatom sources. The decay rate of a complete circular island with attachment/detachment kinetics is $\approx \Gamma \beta / kT$, corresponding to a decay time of $\approx (\rho r^2) / (\Gamma \beta / kT)$. Approximating the Ref. 24 step protrusion as a half circle with a radius of $r \sim 400$ Å, and using parameters derived from our analysis of equilibrium step fluctuations ($\Gamma = 180$ Å³/s, $\beta = 18$ meV/Å), we obtain a decay time of ~ 32 min at $kT = 25$ meV, consistent with the 20-min decay time estimated in Ref. 24.

ACKNOWLEDGMENTS

We thank Ted Einstein, Herbert Pfnuer, and Ellen Williams for many helpful conversations. W. W. Pai and N. C. Bartelt acknowledge support by NSF-MRG Grant No. DMR91-03031. J. E. R. R. acknowledges support by NSF Grants No. CHE-9303062, No. CHE-9157467, the Packard Foundation, and the Sloan Foundation.

- *Present address: Solid State Division, Oak Ridge National Laboratory, Oak Ridge, TN.
- [†]Present address: Sandia National Laboratories, Livermore, CA 94551-0969.
- ¹N. Osakabe, Y. Tanishiro, and K. Yagi, *Surf. Sci.* **109**, 353 (1981).
- ²C. Alfonso, J. M. Bermond, J. C. Heyraud, and J. J. Métois, *Surf. Sci.* **262**, 371 (1992).
- ³E. Bauer, *Ultramicroscopy* **17**, 51 (1985).
- ⁴M. S. Altman, Q. Cai, W. F. Chung, E. Z. Luo, H. Pinkvos, and E. Bauer, in *Metal-Organic Chemical Vapor Deposition of Electronic Ceramics*, edited by S. B. Desu *et al.*, MRS Symposia Proceedings Vol. 335 (Materials Research Society, Pittsburgh, 1994), p. 235.
- ⁵N. C. Bartelt, R. M. Tromp, and E. D. Williams, *Phys. Rev. Lett.* **73**, 1656 (1994).
- ⁶T. A. Land, A. J. Malkin, Y. G. Kuzentsov, A. Mcpherson, and J. J. Deyoreo, *Phys. Rev. Lett.* **75**, 2774 (1995).
- ⁷S.-I. Kitamura, T. Sato, and M. Iwatsuki, *Nature* **351**, 215 (1991).
- ⁸L. Kuipers, M. S. Hodgman, J. W. M. Frenken, and H. Vanbeijeren, *Phys. Rev. B* **52**, 11 387 (1995).
- ⁹M. Poensgen, J. F. Wolf, J. Frohn, M. Giesen, and H. Ibach, *Surf. Sci.* **274**, 430 (1992).
- ¹⁰M. Giesen-Seibert, J. Frohn, M. Poensgen, J. F. Wolf, and H. Ibach, *J. Vac. Sci. Technol. A* **10**, 2597 (1992).
- ¹¹H. J. Zandvliet, B. Poelsema, and H. B. Elswijk, *Phys. Rev. B* **51**, 5465 (1995).
- ¹²B. S. Swartzentruber and M. Schacht, *Surf. Sci.* **322**, 83 (1995).
- ¹³N. C. Bartelt, J. L. Goldberg, T. L. Einstein, E. D. Williams, J. C. Heyraud, and J. J. Métois, *Phys. Rev. B* **48**, 15 453 (1993).
- ¹⁴M. Giesen-Seibert, F. Schmitz, R. Hentjens, and H. Ibach, *Surf. Sci.* **329**, 47 (1995).
- ¹⁵N. C. Bartelt, J. L. Goldberg, T. L. Einstein, and E. D. Williams, *Surf. Sci.* **273**, 252 (1992).
- ¹⁶M. Giesen-Seibert, R. Jentjens, M. Poensgen, and H. Ibach, *Phys. Rev. Lett.* **71**, 3521 (1993).
- ¹⁷L. Masson, L. Barbier, J. Cousty, and B. Salamon, *Surf. Sci. Lett.* **317**, L1115 (1994).
- ¹⁸L. Kuipers, M. S. Hoogeman, and J. W. M. Frenken, *Phys. Rev. Lett.* **71**, 3517 (1993).
- ¹⁹J. S. Ozcomert, W. W. Pai, N. C. Bartelt, and J. E. Reutt-Robey, *Phys. Rev. Lett.* **72**, 258 (1993).
- ²⁰W. W. Pai, N. C. Bartelt, M. Peng, and J. E. Reutt-Robey, *Surf. Sci. Lett.* **330**, L679 (1995).
- ²¹W. W. Pai, N. C. Bartelt, and J. E. Reutt-Robey, following paper, **53**, 15 997 (1996).
- ²²M. Taniguchi, K. I. Tanaka, T. Hashizume, and T. Sakurai, *Surf. Sci. Lett.* **262**, L123 (1992).
- ²³J. Stroscio and D. M. Eigler, *Science* **254**, 1319 (1991).
- ²⁴Recent studies by R. Berndt *et al.*, *Phys. Rev. Lett.* **76**, 1888 (1996), found tip-induced Ag diffusion on the (110) surface with a tunneling voltage ~ 0.37 V and 10 nA, corresponding to a tunneling gap resistance of $\sim 3.7 \times 10^7 \Omega$.
- ²⁵T. A. Jung, R. R. Schlittlers, J. K. Gimzewski, H. Tang, and C. Joachim, *Science* **271**, 181 (1996).
- ²⁶The scaling behavior of equilibrium step fluctuations is valid under two conditions. First, the motion of the step should not be constrained by the neighboring steps. Second, the magnitude of the fluctuations must be of the order of several atomic spacings or larger. When these conditions are not satisfied, one needs to consider the microscopic details of fluctuation mechanisms [see M. Giesen-Seibert and H. Ibach, *Surf. Sci.* **316**, 205 (1994)].
- ²⁷N. C. Bartelt, T. L. Einstein, and E. D. Williams, *Surf. Sci.* **312**, 411 (1994).
- ²⁸The diffusion-limited scenario occurs when the sticking coefficient S for attachment is large (Ref. 15). To estimate s , we use the adatom concentration of 0.05 ML estimated in the following paper, and assume the value of $D \sim 10^{-7} - 10^{-9}$ cm²/s [see C. L. Liu, J. M. Cohen, J. B. Adams, and A. F. Voter, *Surf. Sci.* **253**, 334 (1991)]. The number of attempted hops onto the step edge would then be at least 4×10^5 /s. From the observed attachment rate of 3/s, this implies a sticking coefficient of less than 7×10^{-6} . Such a small coefficient would only affect fluctuations of Fourier components greater than a wavelength of a/S (Ref. 15) (or 40 μ m). Fluctuations of such long wavelength have much larger time constants ($\sim 10^7$ s) than that of our experiment (~ 10 s). Thus, given this scenario, it is unlikely that the small deviations from an exponent of $\frac{1}{2}$ are caused by terrace-limited diffusion. We thus suggest the small, but systematic, lowering of the time exponent is from the contribution of kink motions.
- ²⁹I. Stensgaard, L. Ruan, F. Besenbacher, F. Jensen, and E. Lægsgaard, *Surf. Sci.* **269/270**, 81 (1992).
- ³⁰D. J. Coulman, J. Winterlin, R. J. Behm, and G. Ertl, *Phys. Rev. Lett.* **64**, 1761 (1990).
- ³¹Several “home-built” STM’s are capable of acquiring a 256 points \times 256 points image within 1 sec. For example, the STM designed by Kuipers *et al.* (Ref. 8) is capable of scanning 10^5 pixels per s.
- ³²Since the imaging time scales as q^{-1} and the relaxation time scales as q^{-2} , the “snap shot” condition is valid if $1000/q^2 \gg 18/q$, i.e., $q \ll 50$. We note the wave vector q in Fig. 4(b) is plotted with maximum q , $q = 6$.